

## Noise-aided synchronization of coupled chaotic electrochemical oscillators

István Z. Kiss and John L. Hudson

Department of Chemical Engineering, Thornton Hall, University of Virginia, Charlottesville, Virginia 22903-2442, USA

J. Escalona and P. Parmananda

Facultad de Ciencias, UAEM, Avenida Universidad 1001, Colonia Chamilpa, Cuernavaca, Morelos, Mexico

(Received 19 August 2003; revised manuscript received 3 May 2004; published 19 August 2004)

We report experimental and numerical results on noise-enhanced synchronization of two coupled chaotic oscillators. Enhanced synchronization is achieved through superimposing small-amplitude Gaussian noise on a common system parameter of the two chaotic oscillators. A resonancelike behavior is found: at an optimum level of noise, maximum synchronization is attained. The simulations show that the resonance behavior occurs with both identical and nonidentical oscillators. Noncommon (asymmetric and independent) noise does not enhance synchronization; common noise seems to enhance synchronization.

DOI: 10.1103/PhysRevE.70.026210

PACS number(s): 05.45.Xt, 05.40.-a

### I. INTRODUCTION

Synchronization of chaotic dynamics has been a topic of extensive research during the past decade. Synchronization of complex systems is manifested in different forms: identical [1], phase [2], and generalized [3] synchronization. It has been shown that the different types can be treated in a unified framework [4,5].

Noise can play destructive or constructive roles in the synchronization phenomena of periodic and chaotic oscillators. Above the identical synchronization threshold, i.e., at strong-coupling strengths, noise can induce intermittent desynchronization [6–8]. In contrast, uncoupled periodic [9,10] and chaotic [11,12] oscillators can be identically synchronized with common noise; there exists a threshold value of noise amplitude above which synchronization is obtained. In a recent Letter, the counterplay of weak coupling and weak noise has been shown to enhance phase synchronization of nonidentical chaotic oscillators [13].

In this article, we show the occurrence of resonance behavior in the identical synchronization of moderately coupled chaotic oscillators with the addition of Gaussian white noise. The applied coupling strength is strong enough to cause phase synchronization, but weaker than that required for identical synchronization. It is observed that in this moderately coupled system both constructive (small noise amplitudes) and destructive (large noise amplitudes) effects of noise are important. There exists an optimum level of noise intensity at which maximum synchronization is attained. Noise-induced resonance effects have also been observed in other scenarios, e.g., in amplification of a sub-threshold deterministic signal (stochastic resonance), or noise-induced periodicity (coherence resonance) [14–20].

In this paper, noise-aided synchronization is demonstrated in experiments with two coupled chaotic electrochemical oscillators [21–24]. Noise was added to the system in two different ways: (a) via common external fluctuations in a system parameter (circuit potential) which affects the oscillators equally and (b) via common fluctuations in the coupling strength of the oscillators. These two types of noise are typical of realistic physical systems. The extent of synchroniza-

tion is determined as a function of noise intensity for both types of superimposed noise and their effects are compared. The experimental findings are supported with numerical simulations using a chaotic electrodisolution model. Moreover, in the numerical part of the reported results, we compare resonance curves obtained for different levels of heterogeneity between the two oscillators and we also compare three scenarios for superimposed additive noise in an attempt to elucidate the underlying mechanism of noise-aided synchronization.

### II. EXPERIMENTS

A schematic of the electrochemical system is shown in Fig. 1. A standard electrochemical cell consisting of two nickel working electrodes (Aldrich, 99.99%+, 1 mm diam), a Hg/Hg<sub>2</sub>SO<sub>4</sub>/cc. K<sub>2</sub>SO<sub>4</sub> reference electrode, and a platinum mesh counter electrode is used in the experiments [21]. The distance between the two working electrodes is about 4 mm. The electrodes are embedded in epoxy and reaction takes

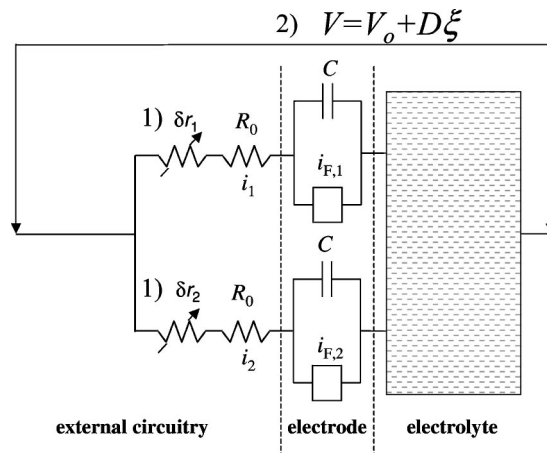


FIG. 1. Schematic of the electrochemical system.

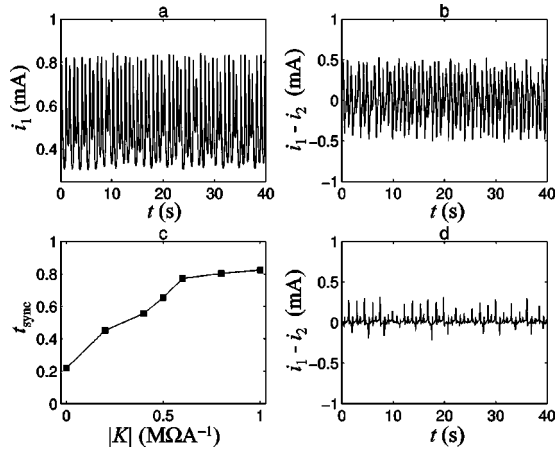


FIG. 2. Experiments: Chaotic dynamics without added noise. (a) Time-series data of currents of one of the electrodes. (b) Time-series data of current differences of two oscillators without coupling ( $K=0 \text{ M}\Omega \text{ A}^{-1}$ ). (c) Synchronization time ( $t_{\text{sync}}$ ) as a function of coupling strength,  $K$ . (d) Time series of current difference at  $K=-1 \text{ M}\Omega \text{ A}^{-1}$ .  $V_0=1.320 \text{ V}$ .

place only at the ends. The electrodes are held at the applied potential (V) with a potentiostat (EG&G PAR 273). Zero-resistance ammeters are used to measure the currents of the electrodes, and data acquisition is done at 200 Hz. The experiments are carried out in 4.5 M sulfuric acid solution at a temperature of 11 °C.

The two electrodes are connected to the potentiostat through two individual parallel resistors,  $R_{1,2}$ . Small perturbations of the resistors ( $R_{1,2}=R_0+\delta r_{1,2}$ ,  $R_0=650 \Omega$ , update frequency 40 Hz, accuracy  $\pm 1.17 \Omega$ ) and the circuit potential ( $V=V_0+\delta V$ , update frequency 200 Hz, accuracy 0.03 mV) are carried out, respectively, by a computer-controlled resistor box (EF-499, Elektroflex) and a 16-bit D/A card.

### A. Effect of coupling without noise

For comparison, we consider first the identical synchronization of two chaotic oscillators without noise. (Similar results under somewhat different conditions can be found in a previous study [22].) Two chaotic oscillators are coupled through the perturbation of individual resistors,

$$\delta r_k(t) = K[i_k(t) - \langle i(t) \rangle],$$

where  $K$  is the coupling strength,  $i_k(t)$  is the current of the  $k$ th electrode, and,  $\langle i(t) \rangle = [i_1(t) + i_2(t)]/2$  is the mean current,  $k=1,2$ . The perturbations are constrained to  $\pm 100 \Omega$  since the experimental setup does not allow the implementation of a wide range of resistor perturbations with high resolution. We apply conditions (Fig. 2) at which the two electrodes exhibit low-dimensional chaotic behavior without added coupling ( $K=0 \text{ M}\Omega \text{ A}^{-1}$ ) [21].

The time series of one of the electrodes and the current difference between the electrodes are shown in Figs. 2(a) and 2(b), respectively. With increasing coupling strength  $K$ , the currents become increasingly synchronized [22]. The extent of identical synchronization is characterized by the synchro-

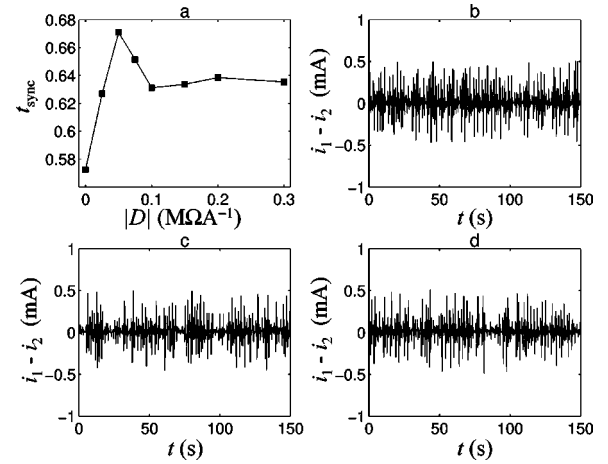


FIG. 3. Experiments: Chaotic dynamics at intermediate coupling strength ( $K=-0.5 \text{ M}\Omega \text{ A}^{-1}$ ) with noise on the coupling strength. (a) The synchronization time ( $t_{\text{sync}}$ ) as a function of noise intensity ( $D$ ). (b) Time-series data of current differences of two oscillators without noise ( $D=0 \text{ M}\Omega \text{ A}^{-1}$ ). (c) Time-series data of current differences of two oscillators at an optimal level of noise intensity ( $D=0.05 \text{ M}\Omega \text{ A}^{-1}$ ). (d) Time-series data of current differences of two oscillators at large noise intensity ( $D=0.2 \text{ M}\Omega \text{ A}^{-1}$ ).  $V_0=1.320 \text{ V}$ .

nization time,  $t_{\text{sync}}$ : the fraction of time in which the two currents are synchronized, i.e., the difference between the currents of the two electrodes, is less than a small value, here 0.05 mA. We have verified that the specific value of this threshold limit within reasonable values does not affect the qualitative results. The chosen value corresponds to about 5% of the size of the attractor. Other measures, such as the standard deviation of the difference between the currents of the electrodes, also gave similar results. The average synchronization time  $t_{\text{sync}}$  [Fig. 2(c)] increases with  $K$ ; the increase becomes small for  $|K| \geq 0.8 \text{ M}\Omega \text{ A}^{-1}$ .

A time series of current differences at  $K=-1 \text{ M}\Omega \text{ A}^{-1}$  shows regions of synchronized behavior and occasional bursts [see Fig. 2(d)]. The differences between the two signals are usually larger at the maxima of the individual oscillations. [At other conditions [22], the bursts are smaller; the bursts in Fig. 2(d) are likely associated with heterogeneity due to surface properties of the metal and/or less precise control of the resistors due to low currents.] Since for  $|K| \geq 0.8 \text{ M}\Omega \text{ A}^{-1}$  further increase in  $t_{\text{sync}}$  is small, we consider the state at  $K=-1 \text{ M}\Omega \text{ A}^{-1}$  to be the experimentally attainable maximal synchronization. To test noise-induced synchronization, we picked a base state corresponding to the situation where the electrodes are synchronized for about 50 % of the time, i.e.,  $K=(-0.5) \text{ to } (-0.4) \text{ M}\Omega \text{ A}^{-1}$ . In this state [the current differences are shown in Figs. 3(b) and 4(b)], not only are the desynchronization amplitudes somewhat larger than at  $K=-1 \text{ M}\Omega \text{ A}^{-1}$  (i.e., in each cycle close to the maximum of the oscillations the differences are larger), but also there are regions in which the elements are not synchronized for a few oscillations. We note that in this base state, due to the moderate coupling, the system is phase-synchronized; the frequency of the two oscillators is equal.

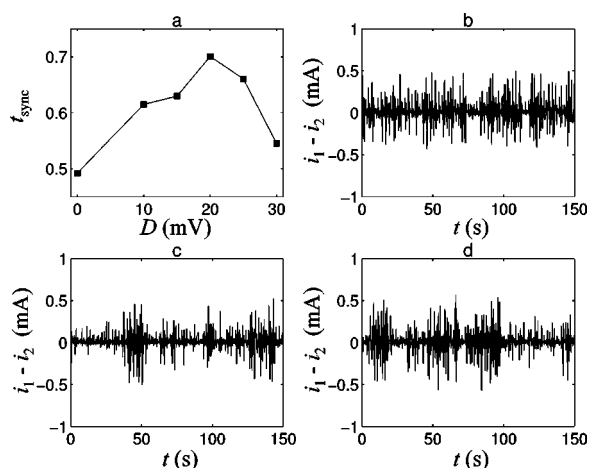


FIG. 4. Experiments: Chaotic dynamics at intermediate coupling strength ( $K=-0.4 \text{ M}\Omega \text{ A}^{-1}$ ) with noise on the potential. (a) The synchronization time ( $t_{\text{sync}}$ ) as a function of noise intensity ( $D$ ). (b) Time-series data of current differences of two oscillators without noise ( $D=0 \text{ mV}$ ). (c) Time-series data of current differences of two oscillators at an optimal level of noise intensity ( $D=20 \text{ mV}$ ). (d) Time-series data of current differences of two oscillators at large noise intensity ( $D=30 \text{ mV}$ ).  $V_0=1.300 \text{ V}$ .

### B. The effect of noise on the coupling strength

We added Gaussian noise to the coupling strength ( $K$ ),

$$K(t) = K_0 + D\xi,$$

where  $\xi$  is Gaussian noise with zero mean and a standard deviation of 1.0;  $D$  is the noise intensity. The synchronization time has a maximum at  $D=0.05 \text{ M}\Omega \text{ A}^{-1}$  [Fig. 3(a)]. At the optimal noise intensity, the oscillators synchronize for longer times [Fig. 3(c)] than with very small (or without) noise [Fig. 3(b)] or with too much noise [Fig. 3(d)]. The increase in synchronization time is small, i.e.,  $t_{\text{sync}}$  increases from 60% without noise to 70% at the optimal noise intensity. (The error of these values is estimated to be about  $\pm 1\%$  based on the analysis of segments consisting of the first and last halves of the data.)

### C. The effect of noise on the circuit potential

We have also explored the effect of adding noise to a common parameter, i.e., the circuit potential

$$V(t) = V_0 + D\xi.$$

With increasing noise intensity we again found an optimal noise strength at which maximal synchrony occurred [Fig. 4(a)]. With too small [Fig. 4(b)] or too large [Fig. 4(d)] noise, the two systems are less synchronized than at optimal noise [Fig. 4(c)]. The synchronization time increases from about 50% to 70% at optimal noise intensity, i.e., the synchronizing effect of noise is stronger through the circuit potential than through the coupling strength.

## III. NUMERICAL RESULTS

To validate the experimental results, numerical simulations were performed using the Koper-Gaspard model [25].

This model reproduces many dynamical features of the chaotic behavior of the nickel electrodisolution and is represented by the following three dimensionless ordinary differential equations:

$$C \frac{de}{dt} = \frac{V-e}{R_0} - 120k(e)u, \quad (1)$$

$$\frac{du}{dt} = -1.25d^{0.5}k(e)u + 2d(w-u), \quad (2)$$

$$\frac{dw}{dt} = 1.6d(2-3w+u), \quad (3)$$

where  $e$  is the double-layer potential,  $C$  is the double-layer capacitance,  $u$  and  $w$  are the concentrations of electroactive species in the so-called ‘‘surface’’ and ‘‘diffusion’’ layers,  $d$  is a transport coefficient, and  $k(e)$  is defined as follows:

$$k(e) = 2.5\theta^2 + 0.01\exp[0.5(e-30)], \quad (4)$$

where  $\theta$  is related to the surface coverage by some (inhibiting) chemical species. The value of  $\theta$  is approximated by the sigmoidal function

$$\theta = \begin{cases} 1 & \text{for } e \leq 35, \\ \exp[-0.5(e-35)^2] & \text{for } e > 35. \end{cases}$$

The dimensionless anodic current is given by  $i_k(t) = [V - e_k(t)]/R_0$ , where  $V$  is the imposed circuit potential ( $V=V_0$  in the absence of noise) and  $R_0$  is the cell resistance. For appropriate parameter values, the model system exhibits a period-doubling route to chaos [25]. We fixed the system parameters at  $(V_0, R_0, d, C) = (36.7395, 0.02, 0.11913, 1)$ , respectively, where low-dimensional chaotic behavior in the anodic current [ $i_k(t)$ ] is observed. The simulations were carried out using a second-order Runge-Kutta integrator with a step size ( $h=0.001$ ); in Sec. III C, a method designed to solve stochastic differential equations [26] was used to prevent stability problems.

### A. The effect of coupling without noise

For two oscillators, Eq. (1) takes the form

$$C_k \frac{de_k}{dt} = \frac{V-e}{R_k} - 120k(e_k)u_k, \quad (5)$$

where  $k=1,2$ .  $C_{1,2} = C \pm \Delta C$ , where  $\Delta C$  is a heterogeneity parameter set to zero unless otherwise noted. As in the experiments, the two chaotic oscillators are coupled through a perturbation of the individual resistors,

$$R_k(t) = R_0 + K[i_k(t-h) - \langle i(t-h) \rangle], \quad (6)$$

where  $K$  is the coupling strength ( $K=K_0$  in the absence of noise) and  $h$  is the step size of the numerical integrator.  $i_k(t) = [V - e_k(t)]/R_k$  is the current of the  $k$ th electrode and  $\langle i(t) \rangle = [i_1(t) + i_2(t)]/2$  is the mean current,  $k=1,2$ . For the numerical simulations, the two uncoupled oscillators ( $R_k = R_0$ ) were left to evolve independently and consequently

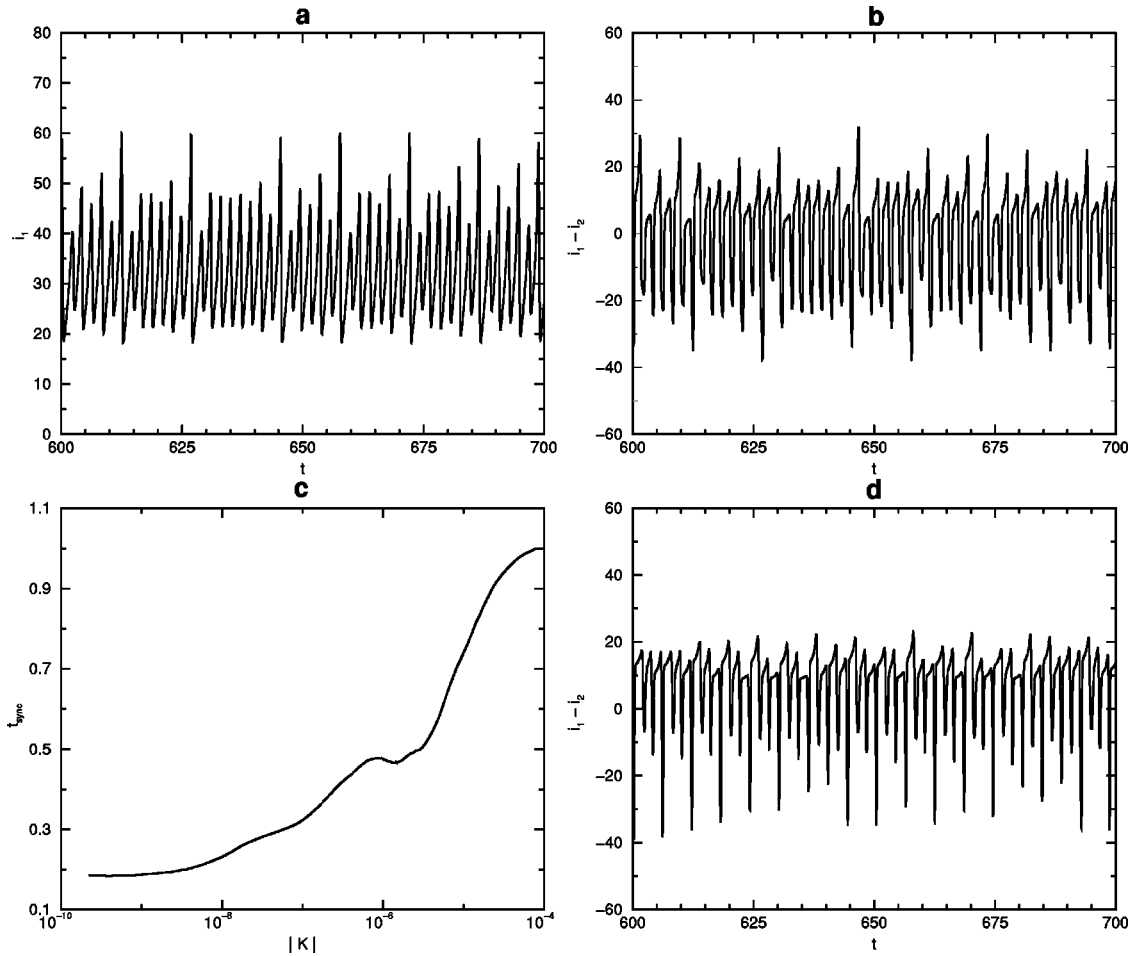


FIG. 5. Numerical simulations: Chaotic dynamics without added noise. The system parameters are  $(V_0, R_0, d, C) = (36.7395, 0.02, 0.11913, 1)$ . (a) Time-series data of currents of one of the oscillators. (b) Time-series data of current differences of two oscillators without coupling ( $K=0$ ). (c) A running average of the synchronization time ( $t_{\text{sync}}$ ) as a function of coupling strength,  $K$ . This average was calculated for 4000 data points using 50 data points as the length of average. (d) Time series of current difference at ( $K=-1 \times 10^{-6}$ ).

$i_k(t) = [V - e_k(t)]/R_0$ . After a sufficiently long time, the coupling was switched “ON”, therefore Eq. (6) should be considered as a recursive relation that enables one to obtain the updated current values in terms of the previous ones. These new current values are subsequently used to calculate the updated values of functions  $e_k$ ,  $u_k$ , and  $w_k$ .

Figures 5(a) and 5(b) show a time series and the difference between two time series for uncoupled chaotic oscillators.

The effect of adding coupling is shown in Fig. 5(c). The extent of synchronization is again characterized by the synchronization time,  $t_{\text{sync}}$ . The dynamics are considered synchronized if the difference between the currents of the two electrodes is less than a predetermined value, in this case 6 (dimensionless current units). The extent of synchronization was also characterized using the standard deviation of the difference between the currents of the electrodes, and results similar to those of Fig. 5(c) were obtained. As is evident from Fig. 5(c), the average synchronization time  $t_{\text{sync}}$  increases with increasing  $|K|$  and identical synchronization occurs for  $|K| > 10^{-4}$ . To test noise-induced synchronization, we picked a base state corresponding to  $K = -1 \times 10^{-6}$  where

the synchronization was observed for about 50% of the time. A time series of current differences under these conditions is shown in Fig. 5(d).

### B. The effect of noise on the coupling strength

Gaussian noise was added to the coupling strength,  $K$ ,

$$K(t) = K_0 + D\xi, \quad (7)$$

where  $\xi$  is Gaussian noise with zero mean and standard deviation of 1.0;  $D$  is the noise intensity. The simulation protocol is similar to the one explained in the previous section (Sec. III A), the difference being that external noise is superimposed. For this set of simulations, the coupling term and the superimposed noise are switched “ON” simultaneously. It needs to be clarified that for this noisy system, the algebraic expressions given by Eq. (6) and (7) are not solved independently but contribute to the right-hand side of the differential equation [Eq. (5)].

We investigated the effect of heterogeneities by systematically varying for different levels of heterogeneities ( $\Delta C$ ). It is evident that the resonance effect diminishes as the het-

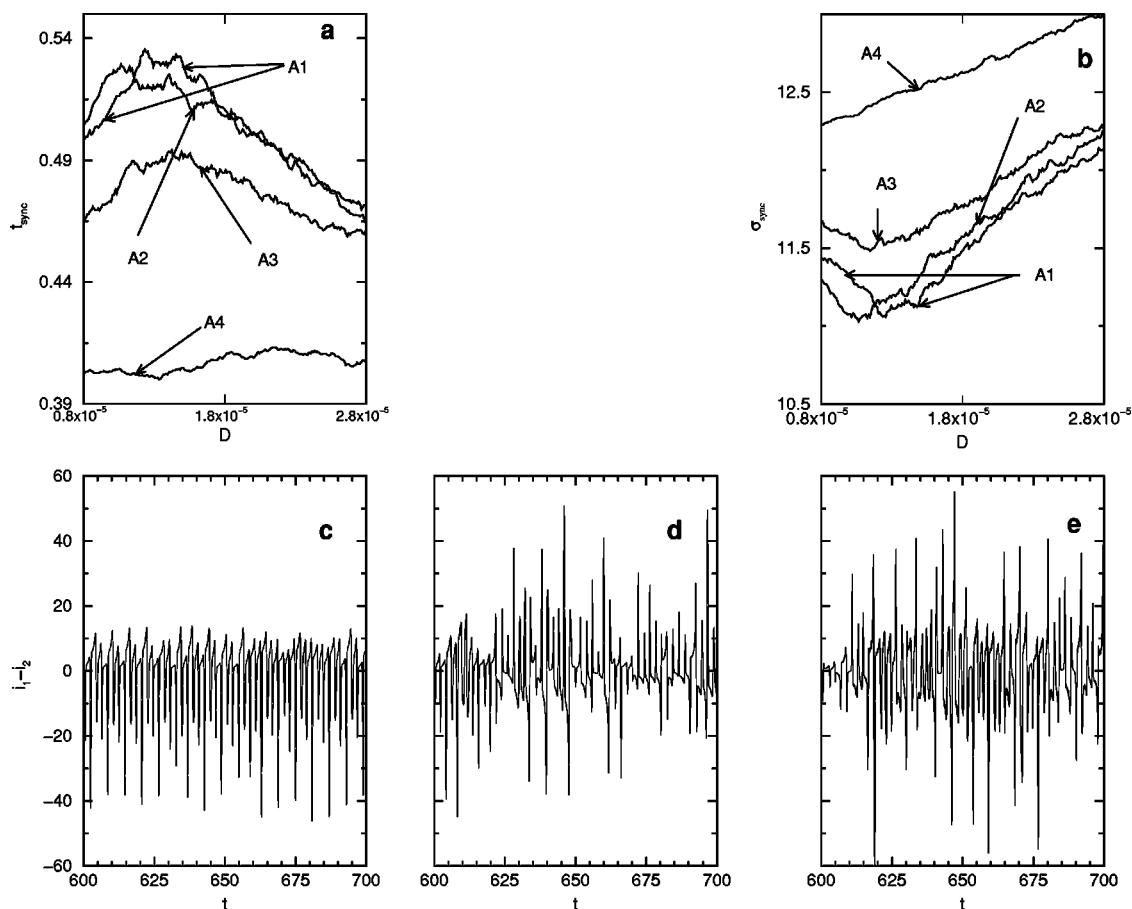


FIG. 6. Numerical simulations: Chaotic dynamics at intermediate coupling strength ( $K = -1 \times 10^{-6}$ ) with noise on the coupling strength. (a) The synchronization time ( $t_{\text{sync}}$ ) as a function of noise intensity  $D$ . Superimposed are resonance curves for different levels of asymmetry between the two electrodes. The curves labeled (A1, A2, A3, A4) correspond to the asymmetry levels  $\Delta C = (0, 5 \times 10^{-4}, 5 \times 10^{-3}, 5 \times 10^{-2})$ , respectively. A running average of  $t_{\text{sync}}$  was computed to suppress local fluctuations and reveal the shape of the resonance curves. This average was calculated for 4000 data points using 50 data points as the length of average. (b) Variance calculation of the individual current difference. A running average of the variance  $\sigma_{\text{sync}}$  was computed to suppress local fluctuations and reveal the shape of the resonance curves. This average was calculated for 4000 data points using 50 data points as the length of average. (c) Time-series data of current differences for two identical oscillators ( $\Delta C = 0$ ) with very little noise ( $D \approx 0$ ). (d) Time-series data of current differences of two oscillators at an optimal level of noise intensity ( $D = 1.23 \times 10^{-5}$ ). (e) Time-series data of current differences of two oscillators at a large noise intensity ( $D = 2.8 \times 10^{-5}$ ).

erogeneity between the oscillators is increased. Moreover, variance calculation of the individual current difference  $[i(2) - i(1)]$  yields consistent results, as shown in Fig. 6(b). Figures 6(c)–6(e) show the time series of differences between the currents of the two oscillators at three distinct values of  $D$  without heterogeneities ( $\Delta C = 0$ ). There is an optimal noise intensity where the oscillators synchronize for longer times [Fig. 6(d)] than with little noise [Fig. 6(c)] or with too much noise [Fig. 6(e)]. The synchronization time increases from 50% without noise to 55% at the optimal noise intensity.

### C. The effect of noise on the circuit potential

Gaussian noise was added to a common parameter, namely the circuit potential,

$$V(t) = V_0 + D\xi. \tag{8}$$

To reiterate, the simulation protocol is identical to the one established in Sec. III B.

Figure 7(a) shows resonance curves for different levels of heterogeneity ( $\Delta C$ ). The resonance effect again diminishes as the heterogeneity is increased. Moreover, variance calculation of the individual current difference  $[i(2) - i(1)]$  yields consistent results, as shown in Fig. 7(b). Figures 7(c)–7(e) show time series of differences between the currents at three distinct values of  $D$  for  $\Delta C = 0$ : The optimal noise intensity case is seen in Fig. 7(d). At the optimal noise intensity, the synchronization time increases to 70% from 50% without noise. As in the experimental observations, we find that the synchronizing effect of noise at optimal intensity is stronger through the circuit potential than through the coupling strength.

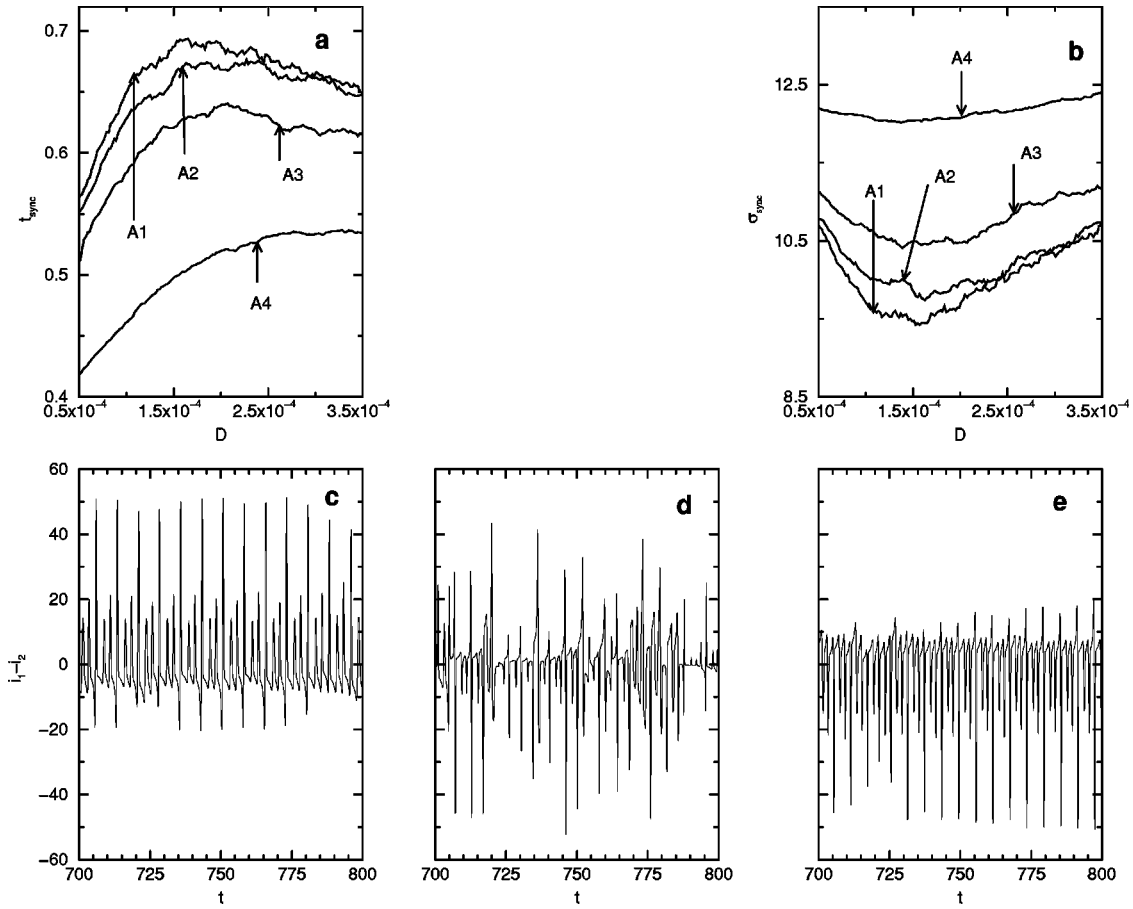


FIG. 7. Numerical simulations: Chaotic dynamics at intermediate coupling strength ( $K = -1 \times 10^{-6}$ ) with noise on the potential (additive noise). (a) The synchronization time ( $t_{\text{sync}}$ ) as a function of noise intensity ( $D$ ). Superimposed are resonance curves for different levels of asymmetry between the two electrodes. A running average of  $t_{\text{sync}}$  was computed to suppress local fluctuations and reveal the shape of the resonance curves. This average was calculated for 4000 data points using 50 data points as the length of average. The curves labeled (A1, A2, A3, A4) correspond to asymmetry levels  $\Delta C = (0, 5 \times 10^{-4}, 5 \times 10^{-3}, 5 \times 10^{-2})$ , respectively. (b) Variance calculation of the individual current difference. A running average of the variance  $\sigma_{\text{sync}}$  was computed to suppress local fluctuations and reveal the shape of the resonance curves. (c). Time-series data of current differences of two identical oscillators ( $\Delta C = 0$ ) with very little noise ( $D \approx 0$ ). (d) Time-series data of current differences of two oscillators at an optimal level of noise intensity ( $D = 1.5 \times 10^{-4}$ ). (e) Time-series data of current differences of two oscillators at a large noise intensity ( $D = 3.5 \times 10^{-4}$ ).

#### D. Effect of noise symmetry on system behavior

Common noise on circuit potential is a symmetric, additive noise; see Eqs. (5) and (8). Common noise on coupling strength is a multiplicative, asymmetric noise; see Eqs. (5)–(7).

In this section, we explore the differences between symmetric and asymmetric noise on the system. For this purpose, we consider only additive noise. To elucidate the role of noise in our moderately coupled chaotic system without heterogeneities ( $\Delta C = 0$ ), we considered three scenarios for the superimposed additive noise on  $V$ : (i) Symmetrical common noise [added to  $V$  as in Eq. (8)]; (ii) asymmetrical common noise ( $V_{1,2} = V_0 \pm D\xi$  for the two oscillators, respectively); and (iii) independent noise ( $V_{1,2} = V_0 \pm D\xi_{1,2}$  for the two oscillators, respectively).

The numerical results of the effect of noise amplitude in the three scenarios are shown in Fig. 8. The addition of common (symmetrical) noise results in a resonance curve with an

increase of synchronization time at moderate noise intensities. When the common noise is added asymmetrically, a very low level of synchronization is observed, and the synchronization time decreases with increasing noise intensity. Independent noise is between the symmetric and asymmetric case; the synchronization time ( $t_{\text{sync}} = 0.47$ ) is somewhat smaller than that of the base case ( $t_{\text{sync}} = 0.5$ ) and it is practically independent of the noise amplitude in the studied range.

The resonance effect is produced by the simultaneous constructive and destructive effects of noise. The symmetric noise acts as a weak effective coupling [29]. This weak effective coupling augments the preexisting coupling ( $K$ ) between the oscillators, and the synchronization time  $t_{\text{sync}}$  increases. However, at higher amplitudes of noise the synchronization degrading effect of noise is observed. When the noise is asymmetric, it apparently introduces an effective negative coupling that decreases the preexisting coupling strength ( $K$ ), and therefore the synchronization times

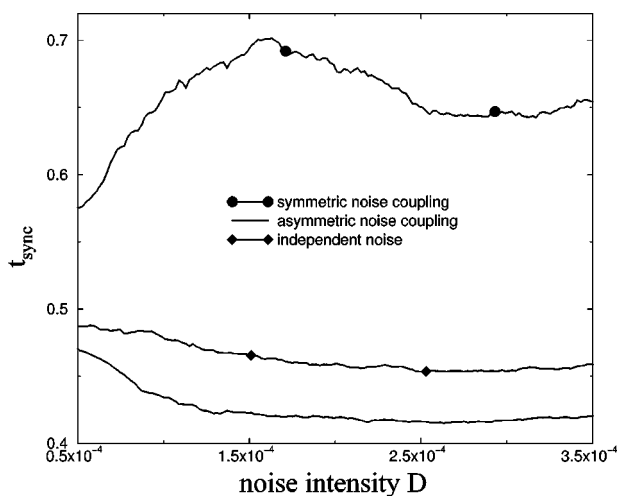


FIG. 8. Numerical simulations: Chaotic dynamics at intermediate coupling strength ( $K=-1 \times 10^{-6}$ ) with noise on the potential (additive noise). The synchronization time ( $t_{\text{sync}}$ ) as a function of noise intensity ( $D$ ) for (a) common noise added symmetrically, (b) common noise added asymmetrically, and (c) independent noise. A running average of  $t_{\text{sync}}$  was computed to suppress local fluctuations in the computed curves. This average was calculated for 4000 data points using 50 data points as the length of average.

$t_{\text{sync}}$  decrease. With independent noise, there is no coupling effect; thus the synchronization properties are practically unaffected.

#### IV. DISCUSSION

Our results indicate that two coupled chaotic systems can exhibit an increased level of synchronization under the influence of common white noise with a Gaussian distribution.

In uncoupled chaotic systems, noise destroys the global chaotic character and produces a complicated, noise-driven

behavior characterized by a negative maximal Lyapunov exponent [11,12,27]. Identical synchronization of two uncoupled chaotic oscillators thus requires a high level of noise intensity. In the moderately coupled chaotic system studied here, however, even small amounts of noise can enhance synchronization and large amounts of noise destroy synchronization. These two effects produce the resonantlike behavior seen here in experiments and simulations. In an experimental system, there is always an intrinsic heterogeneity [24]; we have shown in simulations that the resonant behavior persists even for oscillators with heterogeneities. Two different types of collectivity have been considered. The enhancement of collectivity is more pronounced for noise on a common parameter (such as environmental fluctuations) than on noise via coupling strength. The numerical simulations show that the symmetry of noise is important in noise-aided synchronization; asymmetric noise has a degrading effect and independent noise has a neutral effect. The coupling effect of common noise has been pointed out in weakly coupled oscillators [29] where enhancement of phase synchronization is observed. Here, we have shown that common (symmetric) noise can play an important role in identical synchronization of moderately coupled oscillators.

Our results bear a similarity to an important problem in neuronal spiking: aperiodic perturbations have been shown to increase the replicability of neuronal spike train profiles [28]. So just as in the experiments described here, the addition of a low level of noise can increase correlation between signals.

#### ACKNOWLEDGMENTS

This work was supported by the National Science Foundation (CTS-0000483), the Office of Naval Research (N00014-01-1-0603), and CONACyT (Mexico).

- 
- [1] L. M. Pecora and T. L. Carroll, Phys. Rev. Lett. **64**, 821 (1991).
  - [2] M. G. Rosenblum, A. S. Pikovsky, and J. Kurths, Phys. Rev. Lett. **76**, 1804 (1996).
  - [3] N. F. Rulkov, M. M. Sushchik, L. S. Tsimring, and H. D. I. Abarbanel, Phys. Rev. E **51**, 980 (1995).
  - [4] R. Brown and L. Kocarev, Chaos **10**, 344 (2000).
  - [5] S. Boccaletti, L. M. Pecora, and A. Pelaez, Phys. Rev. E **63**, 066219 (2001).
  - [6] J. F. Heagy, T. L. Carroll, and L. M. Pecora, Phys. Rev. E **52**, R1253 (1995).
  - [7] C. S. Zhou and C. H. Lai, Phys. Rev. E **59**, R6243 (1999).
  - [8] D. J. Gauthier and J. C. Bienfang, Phys. Rev. Lett. **77**, 1751 (1996).
  - [9] A. S. Pikovsky, Radiophys. Quantum Electron. **27**, 576 (1984).
  - [10] R. V. Jensen, Phys. Rev. E **58**, R6907 (1998).
  - [11] C. H. Lai and C. S. Zhou, Europhys. Lett. **43**, 376 (1998).
  - [12] R. Toral, C. R. Mirasson, E. Hernández-García, and O. Piro, Chaos **11**, 665 (2001).
  - [13] C. Zhou, J. Kurths, I. Z. Kiss, and J. L. Hudson, Phys. Rev. Lett. **89**, 014101 (2002).
  - [14] R. Benzi, A. Sutera, and A. Vulpiani, J. Phys. A **14**, 453 (1981).
  - [15] F. Moss, A. Bulsara, and M. F. Shlesinger, J. Stat. Phys. **70**, 1 (1993).
  - [16] P. Jung and G. Mayer-Kress, Phys. Rev. Lett. **74**, 2130 (1995).
  - [17] J. Escalona and P. Parmananda, Phys. Rev. E **61**, 5987 (2000).
  - [18] L. Gammaitoni, P. Hänggi, P. Jung, and F. Marchesoni, Rev. Mod. Phys. **70**, 223 (1998).
  - [19] K. Weisenfeld and F. Moss, Nature (London) **373**, 33 (1995).
  - [20] Arkady S. Pikovsky and Jürgen Kurths, Phys. Rev. Lett. **78**, 775 (1997).
  - [21] I. Z. Kiss, W. Wang, and J. L. Hudson, Phys. Chem. Chem. Phys. **2**, 3847 (2000).
  - [22] I. Z. Kiss, V. Gáspár, and J. L. Hudson, J. Phys. Chem. B **104**,

- 7554 (2000).
- [23] W. Wang, I. Z. Kiss, and J. L. Hudson, *Chaos* **10**, 248 (2000).
- [24] I. Z. Kiss and J. L. Hudson, *Phys. Chem. Chem. Phys.* **4**, 2638 (2002).
- [25] M. T. M. Koper and P. Gaspard, *J. Chem. Phys.* **96**, 7797 (1992).
- [26] H. S. Greenside and E. Helfand, *Bell Syst. Tech. J.* **60**, 1927 (1981).
- [27] A. S. Pikovsky, *Phys. Rev. Lett.* **73**, 2931 (1994).
- [28] Z. F. Mainen and T. J. Sejnowski, *Science* **268**, 1503 (1995).
- [29] C. S. Zhou and J. Kurths, *Phys. Rev. Lett.* **88**, 230602 (2002).